

Soft-Tissue Myxomatous Lesions: Review of Salient Imaging Features with Pathologic Comparison¹

Jonelle M. Petscavage-Thomas,
MD, MPH

Eric A. Walker, MD

Chika I. Logie, MD

Loren E. Clarke, MD

Dennis M. Duryea, DO

Mark D. Murphey, MD

Abbreviations: BPNST = benign peripheral nerve sheath tumor, H-E = hematoxylin-eosin

RadioGraphics 2014; 34:964-980

Published online 10.1148/rg.344130110

Content Codes:    

¹From the Departments of Radiology (J.M.P., E.A.W., D.M.D.) and Pathology (L.E.C.), Penn State Milton S. Hershey Medical Center, 500 University Dr, Room HG300, Hershey, PA 17033; Department of Radiology and Nuclear Medicine, Uniformed Services University of the Health Sciences, Bethesda, Md (E.A.W., M.D.M.); Musculoskeletal Section, American Institute for Radiologic Pathology, Silver Spring, Md (C.I.L., M.D.M.); and Department of Radiology, Walter Reed National Military Medical Center, Bethesda, Md (M.D.M.). Recipient of a Cum Laude award for an education exhibit at the 2012 RSNA Annual Meeting. Received May 25, 2013; revision requested August 15 and received October 25; accepted February 17, 2014. E.A.W. has disclosed financial relationships (see p 977); all other authors have no relevant relationships to disclose. **Address correspondence** to J.M.P. (e-mail: jthomas5@hmc.psu.edu).

TEACHING POINTS

See last page

Myxoid soft-tissue lesions are a heterogeneous group of benign and malignant mesenchymal tumors with an abundance of extracellular mucoid material. These lesions may mimic cysts on radiologic evaluation because of the high water content, and histopathologic features also overlap. Benign myxoid lesions include intramuscular myxoma, synovial cyst, bursa, ganglion, and benign peripheral nerve sheath tumor, including neurofibroma and schwannoma.

Malignant entities include myxoid liposarcoma, myxoid leiomyosarcoma, myxoid chondrosarcoma, ossifying fibromyxoid tumor, and myxofibrosarcoma. Some syndromes are associated with myxoid soft-tissue lesions, such as Mazabraud syndrome in patients with soft-tissue myxomas and fibrous dysplasia. Certain discriminating features, such as intralesional fat in a myxoid liposarcoma, perilesional edema and a rim of fat in soft-tissue myxoma, and the swirled T2-weighted signal intensity and enhancement pattern of aggressive angiomyxoma, assist the radiologist in differentiating these lesions. The presence of an internal chondroid matrix or incomplete peripheral ossification may suggest myxoid chondrosarcoma or ossifying fibromyxoid tumor, respectively. The entering-and-exiting-nerve sign is suggestive of a peripheral nerve sheath tumor. Communication with a joint or tendon sheath and peripheral enhancement may indicate a ganglion or synovial cyst. This article (a) reviews the magnetic resonance, computed tomographic, and ultrasonographic imaging characteristics of soft-tissue myxomatous lesions, emphasizing imaging findings that can help differentiate benign and malignant lesions; (b) presents differential diagnoses; and (c) provides pathologic correlation.

©RSNA, 2014 • radiographics.rsna.org

Introduction

Myxoid tumors of soft tissue are characterized by their mucoid or myxoid extracellular matrix (1), which results in distinctive cross-sectional imaging features. Because of high water content, myxoid lesions tend to resemble fluid, with high-signal-intensity characteristics at T2-weighted magnetic resonance (MR) imaging, low attenuation values at computed tomography (CT), and a hypoechoic to anechoic appearance at ultrasonography (US). Thus, myxoid soft-tissue tumors may be confused with cysts. Although myxoid soft-tissue lesions all contain a myxoid extracellular matrix, they vary considerably in their clinical behavior, ranging from benign to aggressive malignant entities. Benign myxoid lesions include intramuscular myxoma, synovial cyst, bursa, ganglion, and benign peripheral nerve sheath tumors (BPNSTs), such as neurofibroma and schwannoma. Malignant entities include myxoid liposarcoma, myxoid leiomyosarcoma, myxoid chondrosarcoma, ossifying fibromyxoid tumor, and myxofibrosarcoma. It is important to recognize the salient imaging features so that malignant lesions can be differentiated from benign

lesions, thereby preventing unnecessary biopsy and guiding clinical management.

Few articles in the literature have reported on the imaging features of all myxoid soft-tissue lesions. This article reviews the radiologic characteristics of soft-tissue myxomatous lesions, emphasizes imaging findings that may help differentiate benign and malignant lesions, offers differential diagnoses, and provides pathologic comparison.

Benign Lesions

Intramuscular Myxoma

Clinical Features.—Myxoma is a benign mesenchymal neoplasm without malignant potential that is composed of bland undifferentiated stellate cells with thin collagen fibers within a myxoid stroma (2). The reported incidence is one case per 1 million people (3). Myxoma is most frequently diagnosed in patients 40–70 years of age, with a 57% female predilection (4,5). Patients typically present with a slowly enlarging (64%) painful (51%) or painless (49%) soft-tissue mass ranging between 1 and 17 cm in size (6). Intramuscular myxomas are typically solitary. When multiple myxomas are present, they are almost always associated with monostotic or polyostotic fibrous dysplasia, known as Mazabraud syndrome (7,8). Most musculoskeletal myxomas are intramuscular (82%) in location, occurring most often in the thigh (51%), upper arm (9%), calf (7%), and buttock (7%) (8). Management options include observation (because of the benign behavior) or surgical excision, which is typically curative without recurrence (3).

Imaging Features.—Radiographs may demonstrate normal findings (55%) or a nonspecific soft-tissue mass (45%) (6). Bone scintigraphy shows mild or no radionuclide uptake.

US demonstrates a well-defined hypoechoic to near-anechoic mass with some internal echoes and increased through-transmission (Fig 1a) (9–11). Small anechoic cystic areas are present in 85% of cases (6). **A sonographic bright rim sign of increased echogenicity is often noted (in 83% of cases) around the myxoma, which is similar to the rind of fatty tissue around intramuscular myxoma described for MR imaging later. Also frequently noted is the bright cap sign, a triangular hyperechoic area adjacent to at least one of the poles of the mass (12) that corresponds to more prominent adipose tissue at the poles of the lesion.** Color Doppler US shows the lesions to be avascular or hypovascular, with surrounding vessels (3).

Teaching Point

CT typically shows a well-defined homogeneous soft-tissue mass with attenuation higher than that of water and less than that of surrounding muscle (3). Mild diffuse enhancement or peripheral and septal enhancement is seen in approximately 50% of cases (6).

Myxomas demonstrate homogeneous low (81%–100%) to intermediate (0%–19%) signal intensity on T1-weighted MR images (Fig 1b). At T2-weighted MR imaging, all myxomas demonstrate high signal intensity. Lesions are homogeneous or only mildly heterogeneous and are well defined in 60%–80% of cases. In 65%–89% of cases, a thin rim of fat (or approaching adipose tissue signal intensity because of volume averaging) is noted most prominently at the superior and inferior poles of the lesion, representing atrophy of the adjacent muscle. Perilesional high signal intensity may be noted with the use of fluid-sensitive sequences in 79%–100% of myxomas, a finding caused by leakage of the myxomatous tissue into the surrounding muscle (Fig 1c). Both of these findings are unique MR imaging features and may result from the lack of a complete pseudocapsule often seen with myxoma. On contrast material-enhanced MR images, myxomas also usually demonstrate mild (76%) to moderate (24%) contrast enhancement in a diffuse pattern (57%) (Fig 1d) or a thick peripheral and septal enhancement pattern (43%). Cystic areas may be noted in slightly more than 50% of all lesions (6,13–15).

Peripheral Nerve Sheath Tumors

BPNSTs are typically divided into (a) neurofibroma and (b) schwannoma (neurilemoma) (16); both types contain cells closely related to normal Schwann cells.

Neurofibroma.—Neurofibroma accounts for slightly more than 5% of benign soft-tissue tumors (17). Neurofibroma is most commonly seen in patients 20–30 years of age and demonstrates no sex predilection (16,18). Three types of neurofibroma are classically described: localized (90%), diffuse, and plexiform lesions (3). The classic (localized) type is most likely to be confused with a myxoid lesion. Localized neurofibromas are usually slow-growing painless masses measuring as large as 5 cm that often involve the superficial cutaneous nerves, although deep-seated lesions may involve the larger nerves (3). Neurofibromas cannot be separated from the nerve, and complete excision of the neoplasm requires sacrifice of the involved nerve. Thus, deep-seated lesions may only be debulked or observed, to save the nerve. Local recurrence is rare after complete excision.

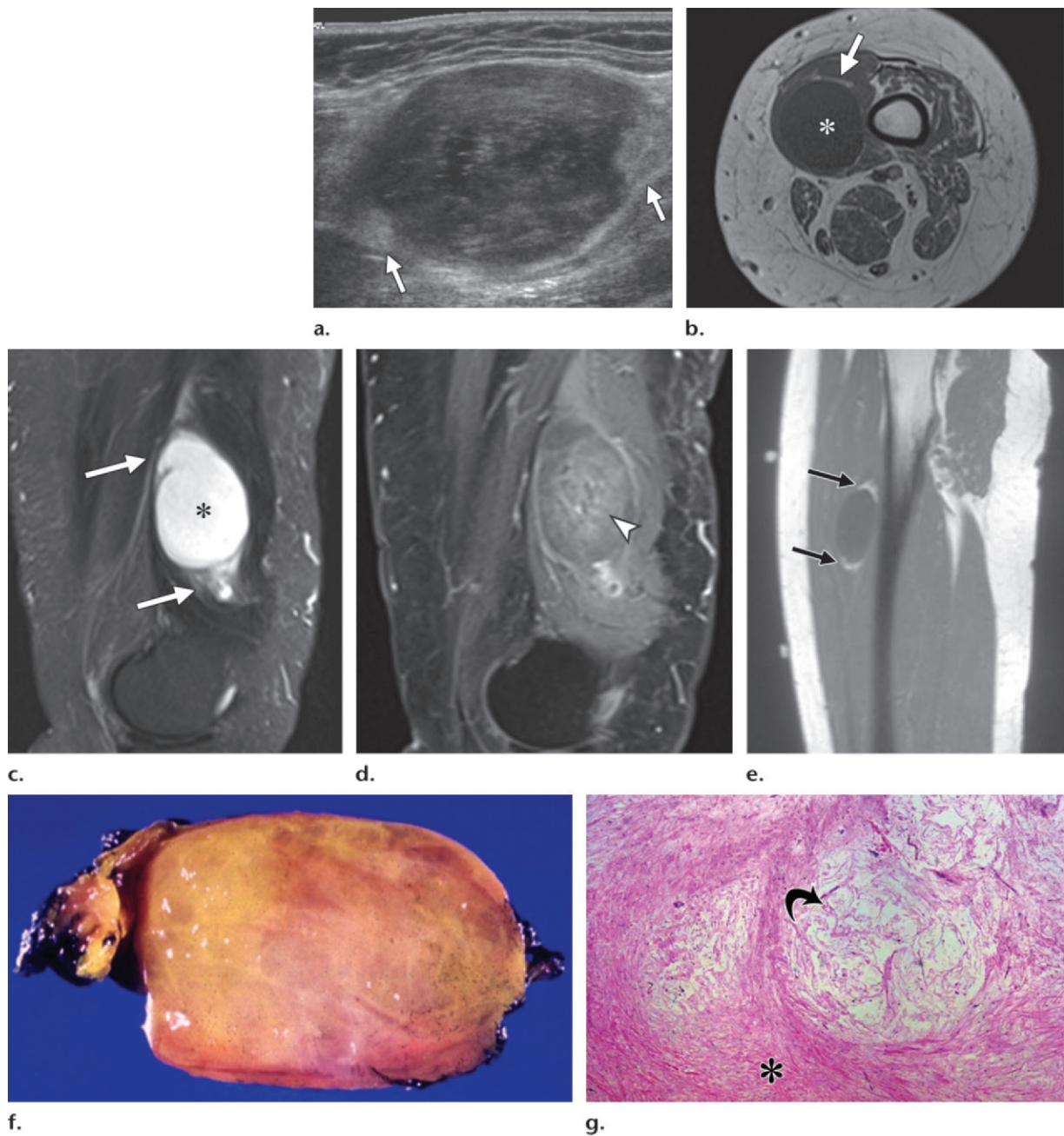


Figure 1. Intramuscular myxoma in a 56-year-old woman with a history of thyroid cancer and an incidental mass noted along the medial distal thigh. **(a)** US image demonstrates an ovoid heterogeneous hypoechoic intramuscular mass. Increased echogenicity at the poles (arrows) represents fat. **(b)** Axial T1-weighted MR image (673/13 [repetition time msec/echo time msec]) demonstrates a homogeneous lesion (*) with low signal intensity relative to that of skeletal muscle and incomplete perilesional fat (arrow). **(c)** Sagittal T2-weighted MR image (7470/100) demonstrates a high-signal-intensity lesion (*) (signal intensity similar to that of water), with peripheral edema most pronounced at the poles (arrows). **(d)** Sagittal contrast-enhanced T1-weighted fat-saturated MR image (1040/13) shows diffuse mild enhancement (arrowhead) of the lesion. **(e)** Sagittal T1-weighted MR image (595/13) of a different patient demonstrates perilesional fat (arrows), which is most pronounced at the poles. **(f)** Photograph of a section of gross specimen demonstrates a gelatinous ovoid mass. **(g)** Photomicrograph (original magnification, $\times 40$; hematoxylin-eosin [H-E] stain) shows undifferentiated spindle cells in a myxoid stroma. A hypocellular hypovascular area (arrow) and an area of increased vascularity and cellularity (*) are shown.

Schwannoma.—Schwannoma (neurilemoma) is slightly less common than neurofibroma and accounts for approximately 5% of all benign soft-tissue tumors (17). Schwannoma is most com-

monly seen in patients 20–50 years of age and demonstrates an equal sex distribution (16,18). Larger lesions or lesions in patients with schwannomatosis may cause pain (3,16). Lesions are

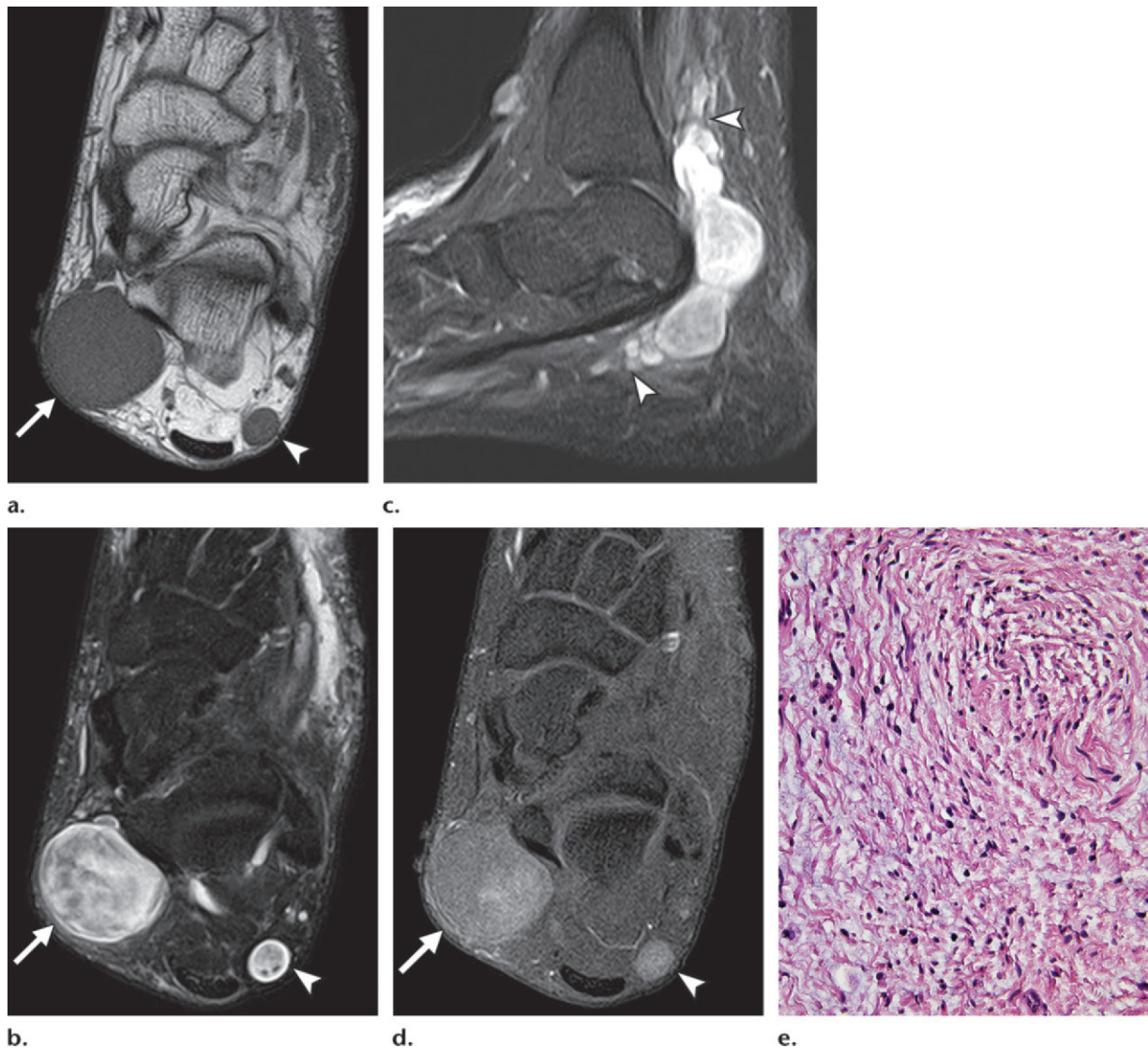


Figure 2. Neurofibromas in a 30-year-old woman with neurofibromatosis type 1 and an enlarging left medial ankle mass. **(a)** Axial T1-weighted MR image (507/10) demonstrates a relatively homogeneous lesion (arrow) and a smaller homogeneous lesion (arrowhead) with signal intensity slightly higher than that of skeletal muscle. **(b)** Axial T2-weighted fat-suppressed MR image (4233/60) demonstrates a heterogeneous high-signal-intensity lesion (arrow) that mimics a cyst. A smaller neurofibroma (arrowhead) demonstrates the more classic target sign, with higher signal intensity at the periphery. **(c)** Sagittal short inversion time inversion-recovery MR image (4700/36) demonstrates a fusiform heterogeneous high-signal-intensity lesion that follows the path of the neurovascular structures with an entering-and-exiting-nerve sign (arrowheads). **(d)** Axial contrast-enhanced T1-weighted fat-suppressed MR image (510/10) shows mild heterogeneous enhancement (arrow, arrowhead) of the lesions. **(e)** Photomicrograph (original magnification, $\times 175$; H-E stain) shows that the tumor is composed of cytologically bland ovoid and spindle cells arranged haphazardly within a myxoid stroma.

most often sporadic (90%) but may be plexiform or multiple in approximately 5% of cases (19,20). Frequent sites of involvement include the cutaneous nerves of the head, neck, and flexor surface of the extremities. Deep-seated lesions are often located in the posterior mediastinum and retroperitoneum (16). Unlike neurofibroma, schwannoma is separable from the adjacent nerve after incision of the epineurium, and the lesion may be removed with preservation of the nerve and its function (3). Recurrence after surgical resection is uncommon, and malignant transformation is rare (3).

BNST Imaging Features.—The most common radiographic abnormality of BNST is a nonspecific soft-tissue mass; in many cases, however, the radiographic findings are normal. On rare occasions, a fusiform soft-tissue mass with surrounding fat is seen. Positron emission tomography with fluorine 18 fluorodeoxyglucose or ^{11}C -methionine has been useful in identifying malignant transformation in patients with neurofibromatosis type 1. As with other soft-tissue neoplasms, BNST is best characterized with cross-sectional imaging (US, CT, and MR imaging).

Figure 3. Neurofibroma of the forearm in a 24-year-old man. **(a)** Radiograph demonstrates the split fat sign (arrows). The split fat sign may be seen with intermuscular lesions. **(b)** Longitudinal color Doppler US image demonstrates a target sign, with lower echogenicity and vascularity of the more myxoid peripheral component. **(c)** Photograph of the sectioned gross specimen demonstrates an entering and exiting nerve (arrows). Unlike the approach with schwannoma, the nerve must be sacrificed for resection of a neurofibroma.



US typically demonstrates a fusiform, well-defined hypoechoic soft-tissue mass, which may have faint distal acoustic enhancement. The presence of a complete or incomplete echogenic rim around the substance of a mass is a rare but nearly pathognomonic feature of nerve tumors. Entering and exiting nerves may be demonstrated. Color Doppler US may be useful in distinguishing the lesion from a ganglion by demonstrating intrinsic blood flow (21).

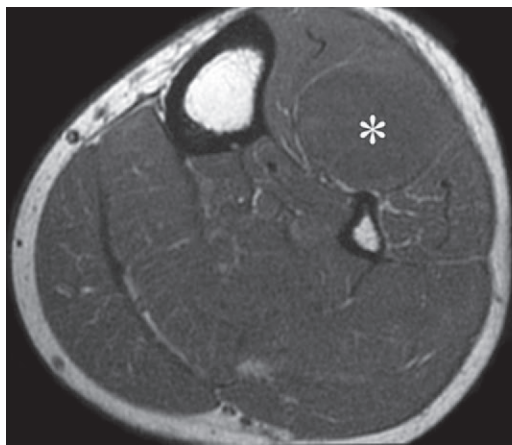
At unenhanced CT, BPNSTs often have low attenuation (as low as 5–25 HU) (22,23), possibly because of high myelin content, entrapped fat, cystic areas, or substantial myxoid tissue with high water content.

At MR imaging, the intrinsic appearance of BPNST is nonspecific, with signal intensity similar to or lower than that of muscle on T1-weighted images and higher than that of fat on T2-weighted images (Fig 2a, 2b). The most important characteristic that suggests BPNST is the fusiform shape caused by the tubular entering and exiting nerve (Fig 2c) (3). With schwannoma, the entering and exiting nerve may be eccentric to the mass. **The target sign is commonly seen in neurofibroma (58%) but can also be detected in schwannoma (15%). This sign refers to low to intermediate T2-weighted signal intensity located centrally secondary to fibrous tissue with a higher collagen content**

and high T2-weighted signal intensity located peripherally, probably related to myxoid (high water content) tissue (24). If the peripheral myxoid component is predominant, the lesion may be confused with other myxoid lesions, particularly on images obtained with fluid-sensitive sequences. The central, more fibrous areas demonstrate avid contrast enhancement in neurofibroma (75%) (Fig 2d) and, less frequently, in schwannoma (8%) (25). A rim of fat (split fat sign) is often seen with deep-seated BPNST, but this sign is nonspecific and can be seen with other intermuscular lesions (Fig 3) (26,27). In our opinion, MR imaging and US are better for demonstrating BPNST, particularly the fusiform shape, because of the improved soft-tissue contrast they provide (27).

Ganglion

Clinical Features.—A ganglion is a tumorlike lesion filled with gelatinous fluid rich in hyaluronic acid and mucopolysaccharides of unknown



a.

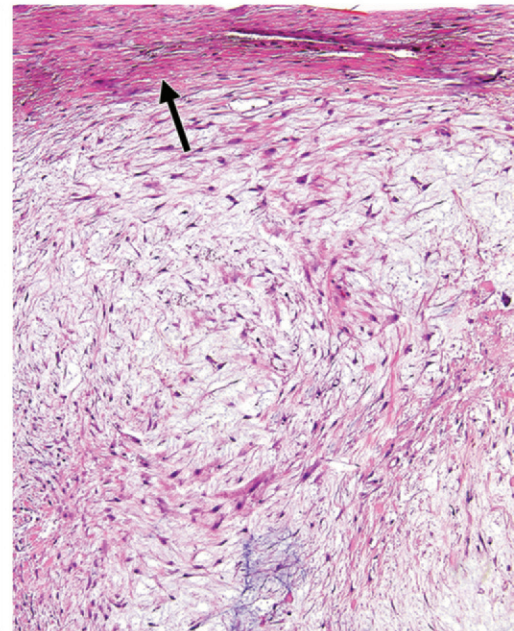
Figure 4. Ganglion in a 54-year-old man with a knee mass and a history of rheumatoid arthritis. **(a)** Axial T1-weighted MR image (516.6/15.4) demonstrates an anterior compartment mass (*) with signal intensity characteristics similar to those of skeletal muscle. **(b)** Sagittal T2-weighted fat-suppressed MR image (2500/70.7) shows a lesion (curved arrow) with internal debris, which appears to originate at the proximal tibiofibular articulation (straight arrow). **(c)** Coronal contrast-enhanced T1-weighted fat-suppressed MR image (750/13.8) demonstrates peripheral and septal enhancement (arrow) of the lesion (*). **(d)** Photomicrograph (original magnification, $\times 175$; H-E stain) shows a dense wall of compact fibrous connective tissue (arrow) surrounding a collection of myxoid material that contains scattered stellate and spindle-shaped cells.



b.



c.



d.

origin that arises in juxta-articular soft tissue. Possible causes include synovial herniation, tissue degeneration, and repeated trauma (28,29). These lesions are often separated into juxta-articular, intra-articular, and periosteal subtypes. We focus on the juxta-articular subtype. Ganglia are common, with 70% located around the wrist; they represent 50%–70% of all soft-tissue masses of the wrist. Most ganglia measure 1.5–2.5 cm. These lesions frequently manifest in adults 25–45 years of age and have a female predilection. Patients may note a palpable mass that is often asymptomatic, but tenderness, pain, or functional impairment is noted in approximately 50% of cases (3). Treatment options include excision, aspiration, and corticosteroid injection.

Imaging Features.—Radiographs may demonstrate normal findings or a soft-tissue mass. US often shows a well-defined homogeneous an-

echoic mass, which may have septa (30) and posterior acoustic enhancement. The lesion is adjacent to a joint or tendon sheath. After aspiration, internal echoes that mimic a solid tumor have been reported (31,32), which represents a potential pitfall. CT demonstrates a juxta-articular lesion of fluid attenuation.

MR imaging most frequently demonstrates a multilobulated mass with homogeneous low T1-weighted and high T2-weighted signal intensity (Fig 4a, 4b). Occasionally, high protein content results in isointense to slightly hyperintense signal intensity with respect to skeletal muscle. T1-weighted MR images often show higher signal intensity than that seen with simple fluid; CT attenuation is frequently higher than 20 HU (20–30 HU), which reflects the high protein content. Peripheral enhancement or peripheral and septal enhancement (of variable thickness but lacking nodularity) is usually noted on contrast-enhanced

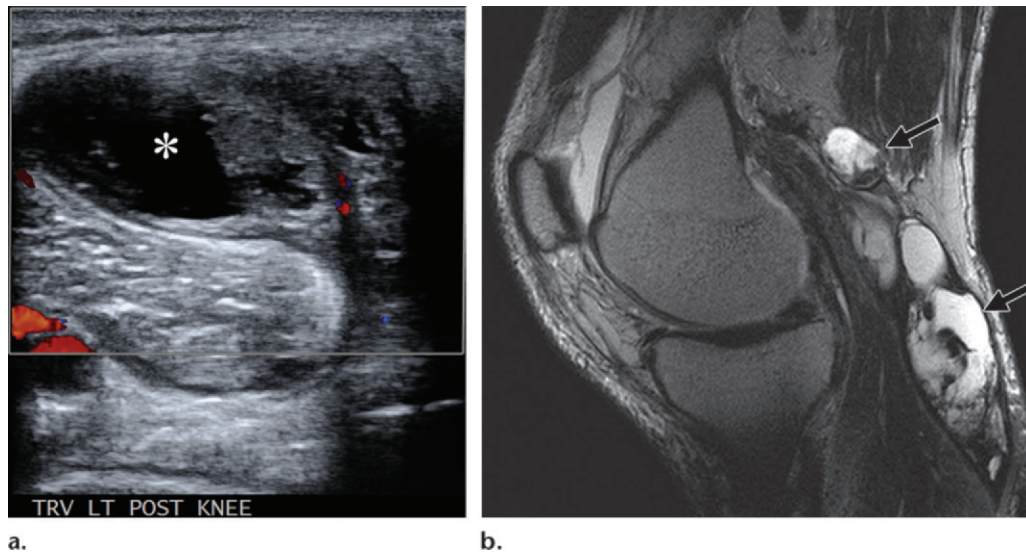


Figure 5. Synovial cyst in a 66-year-old man with left posterior knee pain and a palpable mass. **(a)** Doppler US image demonstrates a hypoechoic heterogeneous lesion with minimal vascular flow within the septa. The mass (*) is medial to the gastrocnemius. **(b)** Sagittal T2-weighted fat-suppressed MR image (2503/65) demonstrates a complex popliteal (Baker) cyst (arrows) with multiple septa and internal debris. The popliteal cyst is the most common of the synovial cysts.

images (Fig 4c). The relationship with the adjacent joint or tendon sheath is best depicted with sequences that have long repetition times and echo times or with gradient imaging sequences (33). It is important to note tails of lesion extension; identifying such extensions assists in complete surgical resection and decreases the incidence of local recurrence. Compression of adjacent nerves may result in atrophy, fatty infiltration, or increased signal intensity of the innervated muscle at T2-weighted imaging (3). Juxta-articular ganglia demonstrate imaging features similar to those of a synovial cyst, often making the two indistinguishable.

Synovial Cyst and Bursa

Clinical Features.—*Synovial cyst* is a term used to describe any synovial-lined juxta-articular fluid collection. It most often represents an extension of joint fluid resulting from chronic effusion. Synovial cysts may be simple, multiloculated, or septated (34). Bursae are synovial-lined cysts that do not normally communicate with a joint. Synovial cysts can arise at any periarticular location, most commonly the knee and hip. The popliteal (Baker) cyst is the most common synovial cyst. Popliteal cysts demonstrate a posterior medial knee fluid collection that communicates with the knee joint between the medial gastrocnemius and semimembranosus tendons. The incidence of popliteal (or Baker) cyst increases with age and in the presence of rheumatoid arthritis or internal derangement

(3). In a study of 1113 patients with internal derangement of the knee, the overall incidence of popliteal cyst was 5% (35). Inflammation from overuse, trauma, internal derangement, infection, or hemorrhage may cause fluid accumulation and thickening of the synovial membrane. Treatment includes observation (because synovial cysts may spontaneously resolve) or aspiration and steroid injection.

Imaging Features.—Radiographic findings for synovial cysts and bursae may be normal or demonstrate a soft-tissue mass or prominence. US shows an anechoic structure communicating with the joint (Fig 5a). The lesion may contain septa, debris, or osteochondral bodies. CT shows a low-attenuation structure adjacent to a joint (synovial cyst) or in an anatomic area subject to friction (bursa). MR imaging usually shows low signal intensity on T1-weighted images, but the signal intensity may be higher if proteinaceous fluid or hemorrhage is present. T2-weighted images show high signal intensity, similar to water. Septa, debris, and osteochondral bodies may be identified (Fig 5b). Enhancement at CT and MR imaging is present only in the lesion wall and possibly within septa in the presence of chronic inflammation or infection. A popliteal cyst rupture can often be demonstrated as edema noted outside of the cyst wall, within the surrounding fascia and soft tissue. The differential diagnosis for popliteal cyst includes bursa, meniscal cysts and ganglia, popliteal artery aneurysm, and deep venous thrombosis.

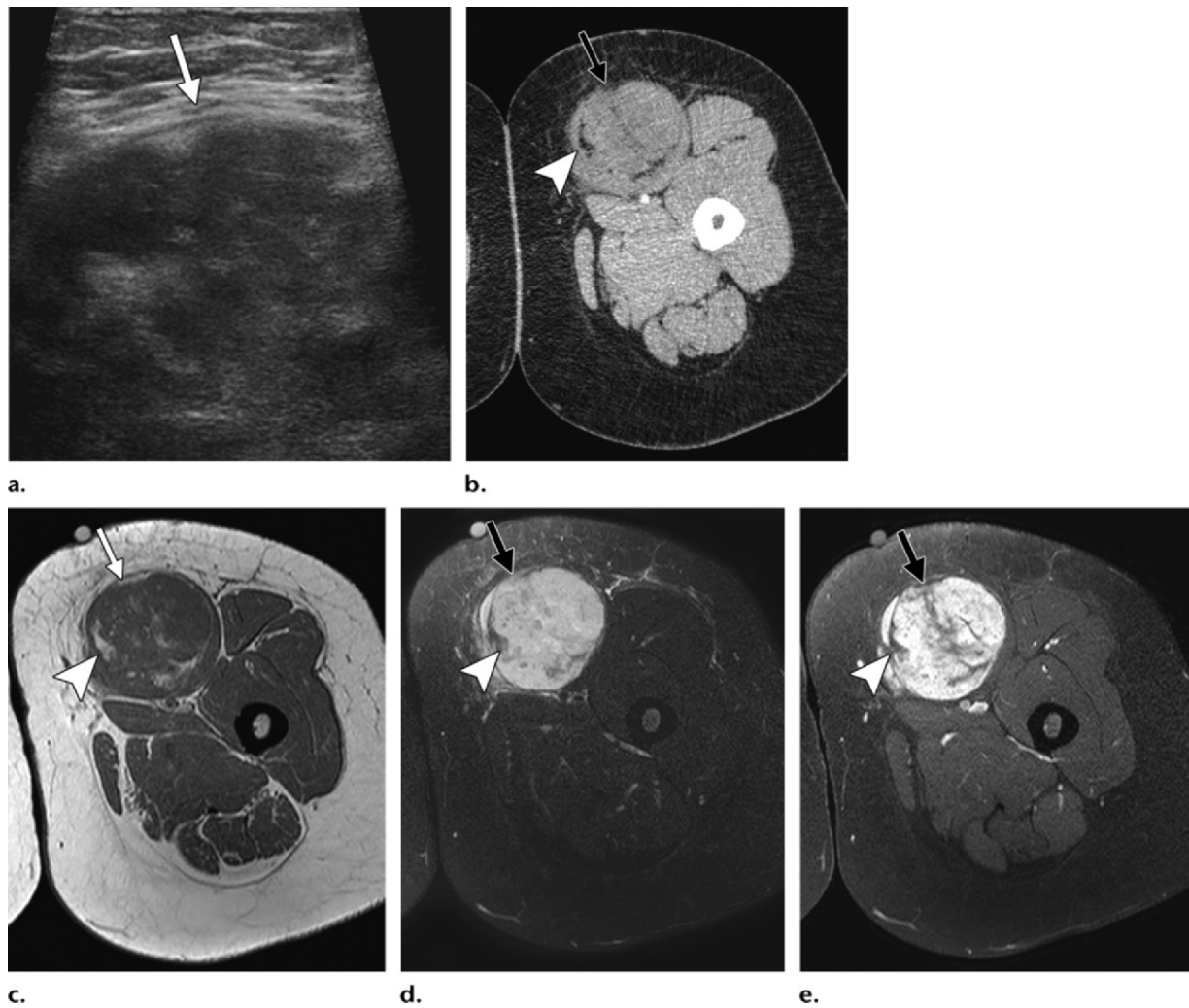


Figure 6. Myxoid liposarcoma in a 48-year-old woman with a left thigh mass that grew slowly during 1 year. **(a)** Transverse US image demonstrates a hypoechoic heterogeneous lesion (arrow) with internal echoes not consistent with a cyst. **(b)** Axial CT image demonstrates a lesion (arrow) with low-attenuation foci (arrowhead), secondary to lipid components. **(c–e)** Axial T1-weighted (746/35) **(c)**, T2-weighted fat-suppressed (5807/70) **(d)**, and contrast-enhanced T1-weighted fat-suppressed (638.3/7) **(e)** MR images show an intramuscular lesion (arrow) with areas of high signal intensity at T1-weighted imaging, low signal intensity with fat saturation, and nonenhancement that correspond to foci of intralesional fat (arrowhead). The lipid component is as much as 10% of the total tumor volume.

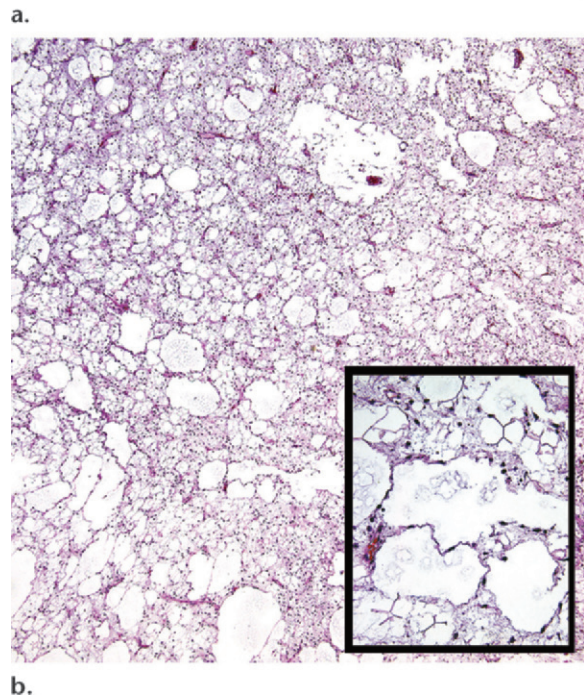
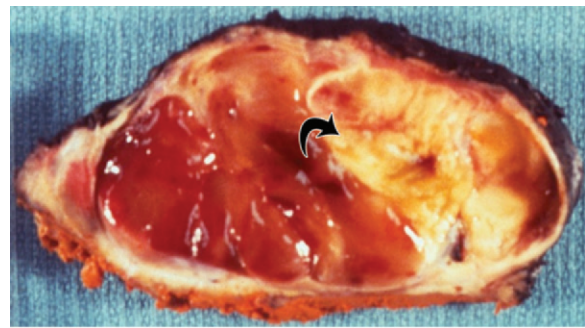
Malignant Lesions

Myxoid Liposarcoma

Clinical Features.—Myxoid liposarcoma is an intermediate- to high-grade malignancy; the grade depends on the percentage of the hypercellular round cell component. Myxoid liposarcoma consists of a myxoid matrix, round or oval primitive nonlipogenic mesenchymal cells, delicate arborizing “chicken wire” vascular networks, and signet ring lipoblasts (4,36). Myxoid liposarcoma is the second most common type of liposarcoma, representing 20%–50% of all liposarcomas and 10% of all soft-tissue sarcomas (37). Myxoid liposarcoma shows no pronounced sex predilection. The lesion occurs

most frequently in patients approximately a decade younger than those affected by other types of liposarcoma, with peak prevalence in the 4th and 5th decades (38). Myxoid liposarcoma most often manifests clinically as a painless soft-tissue mass. Lesions may be large, often larger than 15 cm at presentation. These lesions most often involve the lower extremity (75%–80% of cases), particularly the medial thigh and popliteal locations. Myxoid liposarcomas of the extremities are most frequently intermuscular in location (70%–80% of cases), with intramuscular and subcutaneous locations being less common (38). The lesions have a predilection for extrapulmonary soft-tissue (such as retroperitoneum, opposite extremity, and axilla) or bone (particularly spine) metastases (3,4).

Figure 7. Pathologic features of myxoid liposarcoma in a 28-year-old man with a lateral thigh mass after a motor vehicle accident. **(a)** Photograph of a section of the gross specimen demonstrates a predominantly gelatinous lesion with internal fat (arrow). **(b)** Photomicrograph (original magnification, $\times 40$; H-E stain) shows the classic pulmonary edema pattern, in which adipocyte cytoplasm is markedly expanded and a myxoid stroma predominates. Inset: Photomicrograph (original magnification, $\times 175$; H-E stain) shows cystically dilated spaces lined by thin septa and containing capillary-sized vessels with adjacent smaller adipocytes.



Myxoid liposarcoma is treated with surgical excision, radiation, or adjunct chemotherapy, which is often administered in cases of incomplete or marginal resection (37). The 10-year mortality rate ranges from 30% to 60% and increases with a greater round cell component. Metastatic disease is also more common in myxoid liposarcomas with a larger round cell component. Compared with other subtypes of liposarcoma, myxoid liposarcoma more often has extrapulmonary metastases (37).

Imaging Features.—Radiographs of myxoid liposarcoma may show normal findings but more frequently demonstrate a nonspecific soft-tissue mass. Radiolucent fat is seen much less often in myxoid liposarcoma than in well-differentiated liposarcoma because of a much lower volume of lipid (38). US shows a complex well-defined hypoechoic mass with posterior acoustic enhancement (Fig 6a). The popliteal location of myxoid liposarcomas is common, and such lesions may simulate a popliteal (Baker) cyst (37).

At CT and MR imaging, myxoid liposarcomas are typically large, well-defined multilobulated intermuscular lesions (Figs 6b–6e, 7). The high water content of the lesion is demonstrated as an area of predominant low attenuation on CT images, low signal intensity on T1-weighted MR images, and markedly high signal intensity on T2-weighted MR images (Fig 6b–6d) (38). **The pathognomonic feature of myxoid liposarcoma on MR images is identification of a fatty component within the mass, best seen as foci with high signal intensity on T1-weighted images, usually appearing lacy or linear and amorphous, rather than solid. These foci appear to have intermediate signal intensity with fat-suppressed or short inversion time inversion-recovery sequences (16). MR imaging is superior to CT for the detection of fat because of greater soft-tissue contrast resolution.** Adipose tissue typically constitutes only a small volume of the overall mass (<10% of the lesion) and is often noted within septa (lacy or linear pattern) or as subtle

small nodules. Fat is demonstrated in as many as 90%–95% of myxoid liposarcomas at MR imaging (37). Myxoid liposarcoma often demonstrates intense enhancement. The enhancement pattern can be classified into three groups: homogeneous (total enhancement), heterogeneous (partial enhancement and often more prominent peripherally) (Fig 6e), and no enhancement (3.7%) (16). Comparing the images obtained with T1- and T2-weighted (or T2-weighted fat-saturated) sequences in the same section can be useful to identify subtle fat in the septa.

Myxofibrosarcoma

Clinical Features.—Myxofibrosarcoma (the lesion formerly known as myxoid malignant fibrous histiocytoma) varies from a hypocellular, mainly myxoid, and purely spindle cell appearance (low-grade neoplasms) to a higher-grade pleomorphic lesion (malignant fibrous histiocytoma-like) with multinucleate giant cells, high mitotic activity, and areas of necrosis (39). Myxofibrosarcoma is a common soft-tissue sarcoma in elderly patients (median age,

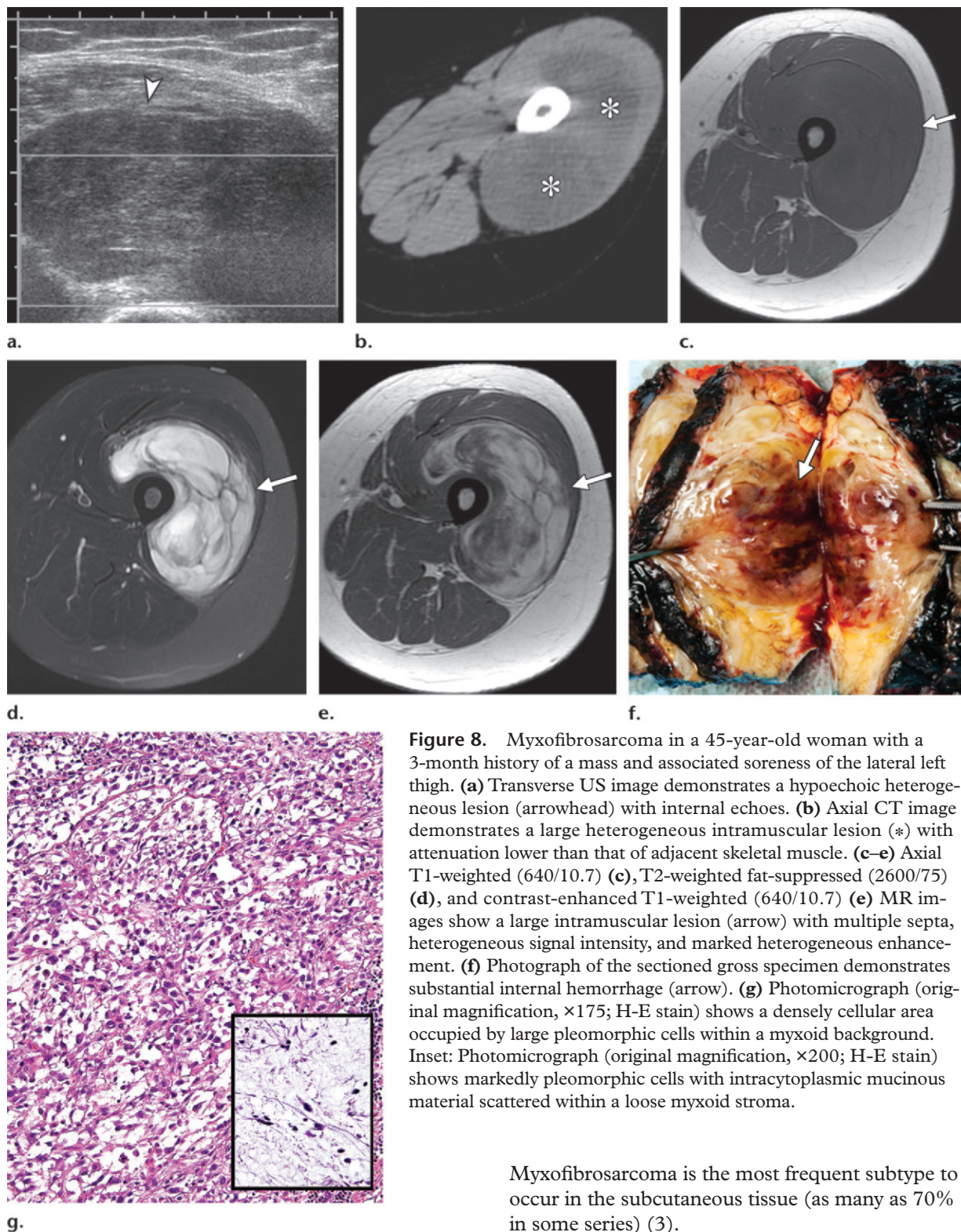


Figure 8. Myxofibrosarcoma in a 45-year-old woman with a 3-month history of a mass and associated soreness of the lateral left thigh. (a) Transverse US image demonstrates a hypoechoic heterogeneous lesion (arrowhead) with internal echoes. (b) Axial CT image demonstrates a large heterogeneous intramuscular lesion (*) with attenuation lower than that of adjacent skeletal muscle. (c–e) Axial T1-weighted (640/10.7) (c), T2-weighted fat-suppressed (2600/75) (d), and contrast-enhanced T1-weighted (640/10.7) (e) MR images show a large intramuscular lesion (arrow) with multiple septa, heterogeneous signal intensity, and marked heterogeneous enhancement. (f) Photograph of the sectioned gross specimen demonstrates substantial internal hemorrhage (arrow). (g) Photomicrograph (original magnification, $\times 175$; H-E stain) shows a densely cellular area occupied by large pleomorphic cells within a myxoid background. Inset: Photomicrograph (original magnification, $\times 200$; H-E stain) shows markedly pleomorphic cells with intracytoplasmic mucinous material scattered within a loose myxoid stroma.

66 years). The incidence is approximately equal in men and women (39). Patients typically present with a slowly enlarging painless mass. Local recurrences occur in as many as 50%–60% of cases (4). Frequent sites of involvement include the extremities (77%), trunk (12%), retroperitoneum or mediastinum (8%), and head (3%) (40,41).

Myxofibrosarcoma is the most frequent subtype to occur in the subcutaneous tissue (as many as 70% in some series) (3).

Treatment involves preoperative chemotherapy, followed by wide en bloc resection (3). The 5-year survival rate for patients with myxofibrosarcoma is 60%–70%, with a 50%–70% local recurrence rate and a 23%–30% metastatic rate (3).

Imaging Features.—Radiographs of soft-tissue myxofibrosarcoma may demonstrate a soft-tissue mass. US, CT, and MR imaging frequently

demonstrate, respectively, predominant low echogenicity, low attenuation, and low signal intensity areas on T1-weighted images, reflecting the high water content of the myxoid component (Fig 8). Higher-grade lesions may demonstrate attenuation at CT similar to that of muscle. T2-weighted MR images show high signal intensity. Heterogeneity is often noted with all MR pulse sequences, reflecting the considerable histologic variability within these lesions. The more cellular areas, often nodular and peripheral, demonstrate enhancement; however, diffuse lesion enhancement may be present in higher-grade lesions with more vascularized myxoid tissue (3). **Myofibrosarcoma is most difficult to distinguish from myxoid liposarcoma. Hemorrhage on T1-weighted images may mimic intralesional fat but has high signal intensity on T1-weighted fat-suppressed images.**

Myxoid Chondrosarcoma

Clinical Features.—Myxoid chondrosarcoma is a rare histologic variant (<2% of all soft-tissue sarcomas) (42,43) of chondrosarcoma that occurs in both soft tissue and bone. Myxoid chondrosarcoma is considered an intermediate-grade tumor. These lesions have high water content, related to the extensive myxoid stroma and areas of hyaline cartilage (44). This lesion was originally called “chordoid sarcoma” on the basis of its histologic resemblance to chordoma (45). Myxoid chondrosarcoma grows slowly and is late to metastasize, with 10-year survival rates ranging from 65% to 78% (46–48).

Extraskelatal myxoid chondrosarcoma is the most common histologic type of soft-tissue chondrosarcoma. It is a tumor that occurs predominantly in adults, with a mean age at presentation of 50 years, although patient age ranges from 4 to 92 years (44). In most but not all series, a male predominance is reported. Extraskelatal myxoid chondrosarcoma is extremely rare in patients younger than 20 years of age (44,49). The most common manifestation is an enlarging soft-tissue mass, but some lesions are accompanied by pain and tenderness (50). Most lesions arise in the extremities, with the thigh being the single most common location. Lesions most frequently affect the deep soft tissues, although approximately 25%–33% of the lesions are subcutaneous (44,51). Treatment involves surgical excision (50). Extraskelatal myxoid chondrosarcoma demonstrates frequent recurrences and metastases, and long-term follow-up is needed (50).

Imaging Features.—Radiographs of these lesions often demonstrate a nonspecific soft-tissue mass. Areas of chondroid matrix mineralization

may be apparent. Underlying bone erosion or invasion and periosteal reaction are unusual but may be seen (44).

Reflecting its extremely high water content, extraskelatal myxoid chondrosarcoma appears as areas of low attenuation on CT images and high signal intensity on T2-weighted MR images (Fig 9a, 9c), with only mild peripheral to septal enhancement after administration of contrast material. Lobular growth, which is typical of chondroid neoplasms, is also frequently apparent. Areas of hemorrhage are also common compared with other chondroid lesions. CT may demonstrate a chondroid matrix (Fig 9a) (44).

Myxoid Leiomyosarcoma

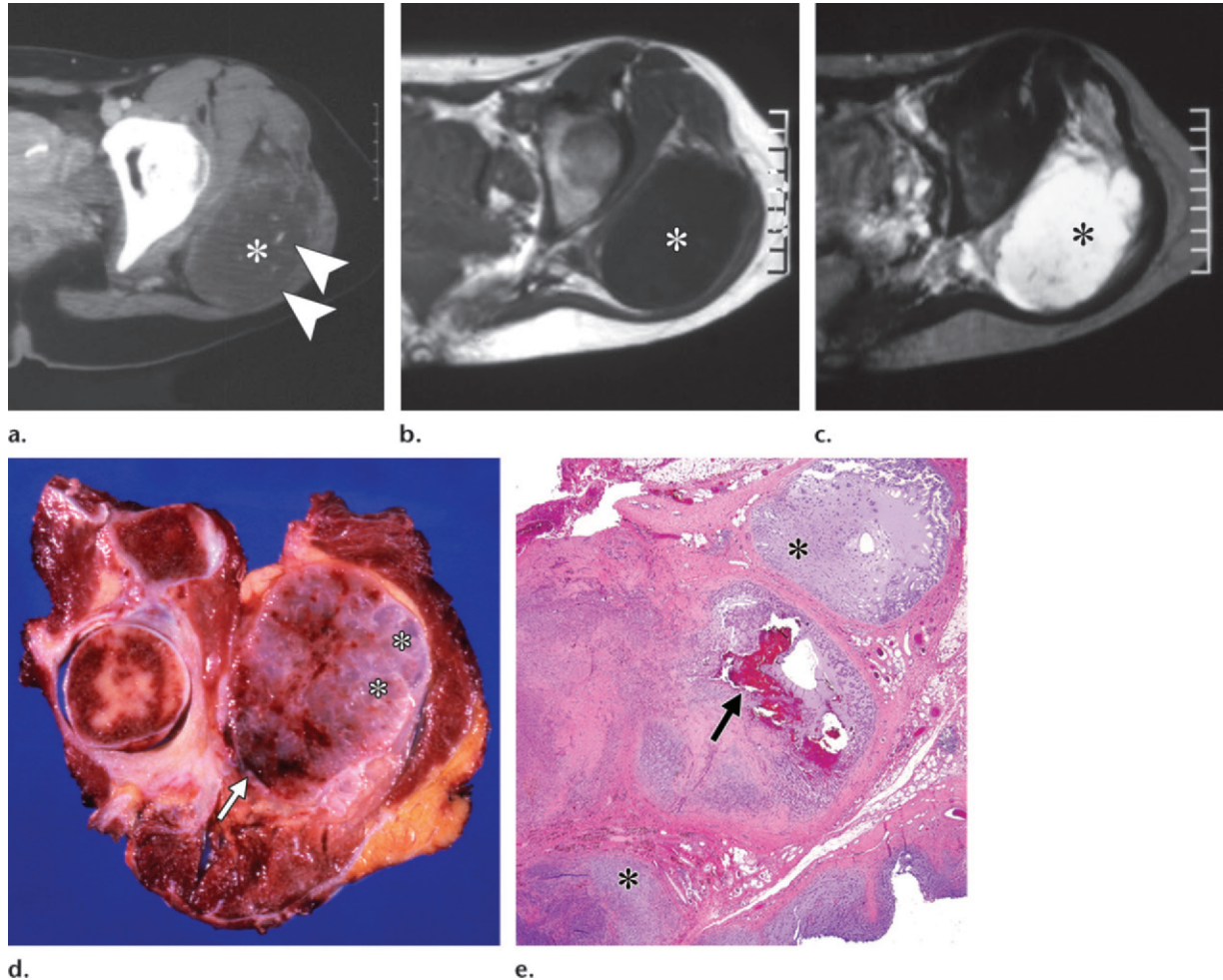
Clinical Features.—Myxoid leiomyosarcoma is a rare variant of leiomyosarcoma, which is found in the genital tract (uterus), retroperitoneum, and, less commonly, the thigh (52). Myxoid leiomyosarcoma is the most common soft-tissue sarcoma of the gastrointestinal tract and uterus, and the median patient age is 60 years (53). Myxoid leiomyosarcomas contain abundant myxoid material between smooth muscle cells. Histologically, the lesion is composed of spindle-shaped cells with a fascicular, reticular, or myxofibrosarcoma-like architecture (1). Treatment involves surgical excision. In a series of 14 myxoid liposarcomas, mitotic activity and grade were lower than those of conventional leiomyosarcoma (54). However, as with conventional leiomyosarcoma, myxoid variants do have local recurrence (36%) and metastases (14%) (54).

Imaging Features.—As seen with other myxoid soft-tissue lesions, low to intermediate signal intensity on T1-weighted images and markedly high signal intensity on T2-weighted images, features that correspond to the myxoid component, are seen at MR imaging (Fig 10). Attenuation similar to that of muscle is seen at CT. Delayed diffuse enhancement or a reticular pattern of enhancement due to the myxoid content can be seen with myxoid leiomyosarcoma (54).

Ossifying Fibromyxoid Tumor

Clinical Features.—Ossifying fibromyxoid tumor is a rare intermediate-grade malignant soft-tissue tumor that typically manifests as a slow-growing painless firm area of subcutaneous swelling or, rarely, a deeper soft-tissue mass (55). The tumor measures from less than 5 cm to 10 cm, is primarily found in the extremities, and is seen more often in men in the 5th decade of life (56–58). Ossifying fibromyxoid tumor is less commonly found in the trunk (16%–19%) and the head and

Figure 9. Myxoid chondrosarcoma in a 50-year-old woman with a gluteal mass. **(a)** Axial CT image shows subtle chondroid matrix mineralization (arrowheads) in a low-attenuation gluteal mass (*). **(b)** Axial T1-weighted MR image (500/25) demonstrates the low-signal-intensity mass (*). **(c)** Axial T2-weighted fat-saturated MR image (3000/80) demonstrates the markedly high signal intensity of the mass (*), with lobular growth best seen anterolaterally. Matrix mineralization cannot be seen on the MR images. **(d)** Photograph of an axial section of the gross specimen demonstrates high-water-content myxoid and cartilaginous (*) nodules and a hemorrhagic focus (arrow). **(e)** Photomicrograph (original magnification, $\times 40$; H-E stain) shows chondroid nodules (*) surrounded by fibrous septa. Hemorrhage (arrow) is prominent in some areas.



neck (9%–13%) (3). Histologically, both a myxoid stroma and a fibrous stroma are seen, which can resemble myxoid chondrosarcoma (55). Local recurrence occurs in 17%–27% of patients after complete surgical excision, whereas metastases are uncommon (5%) (3).

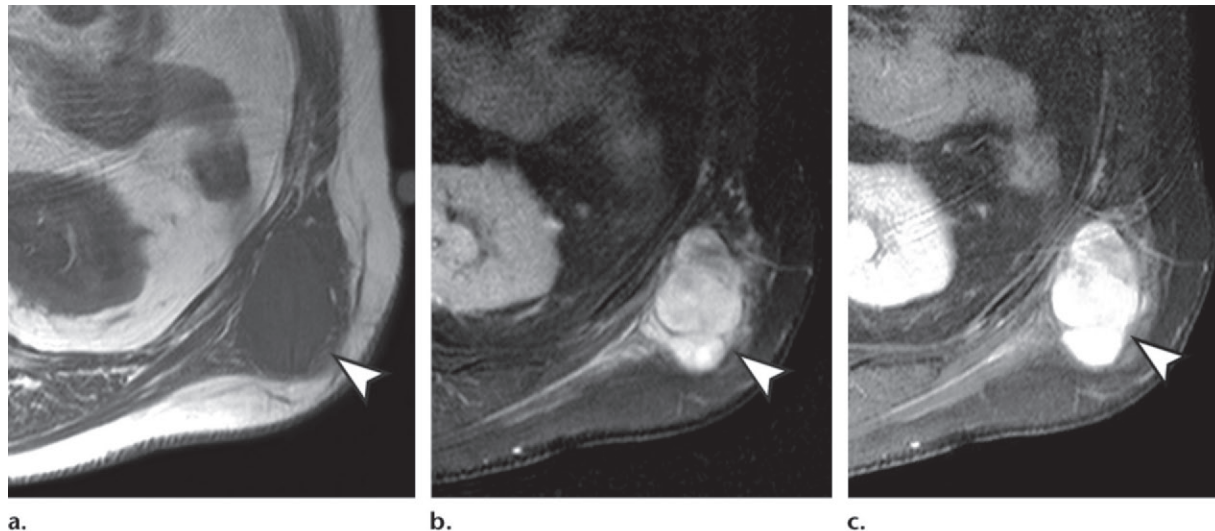
Imaging Features.—Radiographs may demonstrate a small well-defined subcutaneous mass with a peripheral incomplete rim of ossification (this appearance can simulate myositis ossificans), no mineralization, or extensive mineralization (3,59). Heterogeneous uptake has been seen at bone scintigraphy, representing osteoblastic activity (59,60). CT is helpful in showing the surrounding or intralesional ossification without adjacent osseous reaction (60) (Fig 11a). These areas of ossification ap-

pear as areas of low signal intensity on both T1- and T2-weighted MR images, whereas the myxofibrous component is isointense to muscle on T1-weighted images and has intermediate to high signal intensity on T2-weighted images (Fig 11b). Areas of high signal intensity on both T1- and T2-weighted images can be seen if there is internal hemorrhage, which can mimic the fat of a myxoid liposarcoma.

Aggressive Angiomyxoma

Clinical Features.—Aggressive angiomyxoma is an uncommon mesenchymal tumor composed of scattered spindle cells and abundant medium-sized vessels within a myxoid matrix (61). The lesion predominantly occurs in women (90%) (62). The age range is 16–70 years, with a

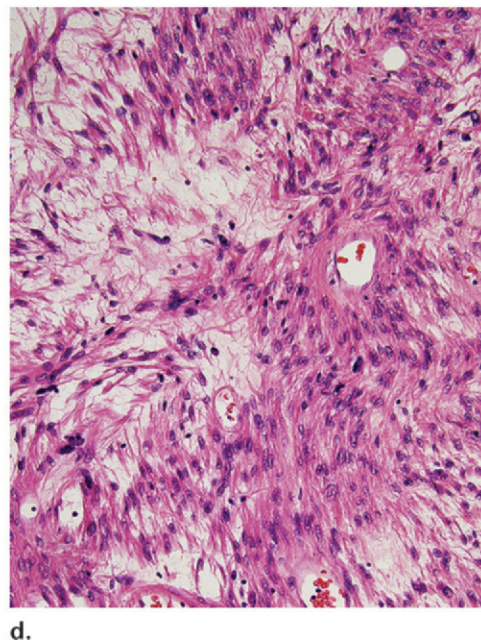
Figure 10. Myxoid leiomyosarcoma in a 72-year-old man with a chest mass. **(a)** Axial T1-weighted MR image (500/20) demonstrates a low-signal-intensity round mass (arrowhead) in the subcutaneous tissue of the upper left abdominal wall. **(b)** Axial T2-weighted MR image (2489/70) shows an area of markedly high signal intensity (arrowhead) due to the myxoid content of the lesion. **(c)** Axial contrast-enhanced T1-weighted fat-suppressed MR image (525/20) demonstrates diffuse enhancement of the anterior aspect of the mass (arrowhead). **(d)** Photomicrograph (original magnification, $\times 200$; H-E stain) shows that the tumor is composed of aggregates of elongated ovoid cells separated by large zones of myxoid material.



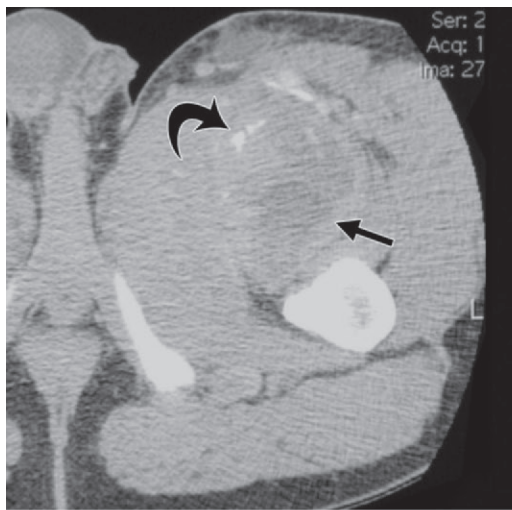
median age of 34 years (62). Aggressive angio-myxomas arise from connective tissues of the perineum or lower pelvis but only rarely occur directly from any pelvic or perineal viscus (63,64). These lesions may be asymptomatic or may cause pain and dyspareunia (3). Aggressive angio-myxomas typically involve the soft tissues of the pelvis, perineum, vulva, buttock, retroperitoneum, and inguinal regions. Most of these tumors are as much as 10 cm in size at manifestation (62), although they can become large (20 cm) (3). Wide excision is the treatment of choice (3). Metastases of aggressive angio-myxoma have not been reported, but the tumor is probably called “aggressive” because of the high rate of local recurrence (36%–72%) after resection (62,65). The lesion is included in the malignant section because of its high local recurrence rate, but many would consider it benign.

Imaging Features.—Radiographs can have normal findings or show a nonspecific soft-tissue mass with displacement of pelvic structures. At US, the lesion may appear hypoechoic or cystic (63,64).

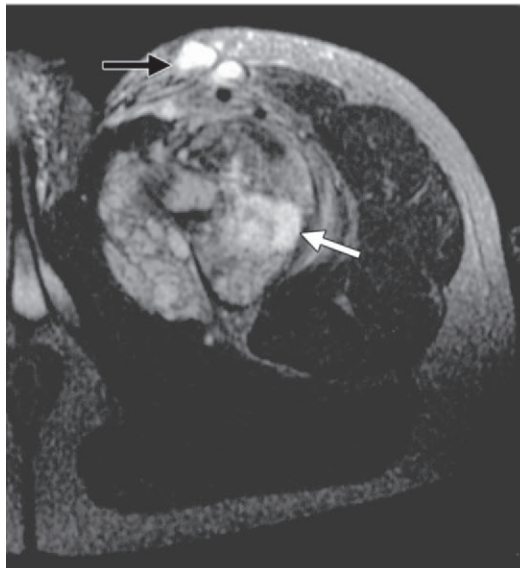
At CT, the lesion has a well-defined margin and attenuation less than that of skeletal muscle (Fig 12a). A swirled appearance may be noted on contrast-enhanced images because intravenous contrast material enhances the strands of fibrovascular tissue within the tumor (61). Aggressive angio-myxoma tends to grow around the structures of the pelvic floor without penetrating the muscularis of the vagina or rectum (66,67).



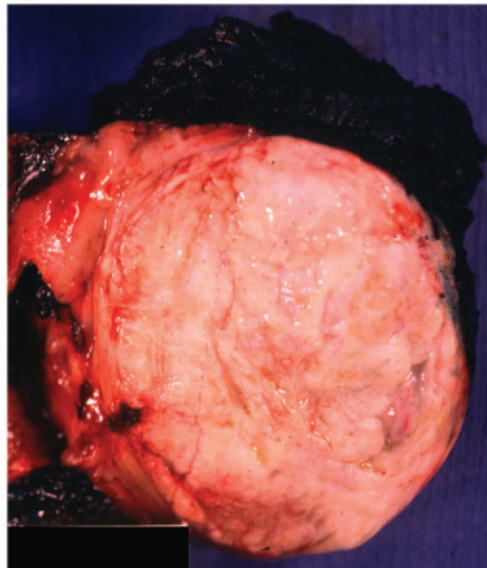
On T1-weighted MR images, this lesion is usually low to intermediate in signal intensity (3). On T2-weighted images, the lesion demonstrates high signal intensity, probably related to the high water content of the loose myxoid matrix. **Aggressive angio-myxoma may demonstrate swirled or layering tissue, seen best with sagittal T2-weighted MR sequences (Fig 12b) but also noted at CT and T1-weighted MR imaging after administration of contrast material (83%), resulting in a distinctive appearance (Fig 12c) (3,61).** These lesions demonstrate a tendency to displace rather than invade perineal structures. Extension from the perineum



a.



b.



c.

Figure 11. Ossifying fibromyxoid tumor in a 41-year-old man who had a left inguinal mass for 7 months. **(a)** Axial CT image shows a soft-tissue mass (straight arrow) in the anterior compartment of the proximal left thigh with heterogeneous attenuation and an incomplete rind of peripheral ossification (curved arrow). **(b)** Axial T2-weighted MR image (4400/66) of the thigh shows areas of high signal intensity (white arrow) due to the myxoid component and peripheral low signal intensity due to ossification. Two pathologic high-signal-intensity lymph nodes (black arrow) are seen anteriorly. **(c)** Photograph of a section of the gross specimen demonstrates a multinodular surface with areas of cystic degeneration.

across the pelvic diaphragm into the pelvis is common and often clinically unsuspected (61), but it must be identified to guide surgical resection. The differential diagnosis includes myxoid liposarcoma and infiltrating angioliipoma.

Conclusions

Myxoid lesions all share the same mucoid extracellular matrix, which results in a hypoechoic US appearance, low attenuation at CT, and high signal intensity with long-repetition-time MR imaging sequences, mimicking a cyst. Certain discriminating features, such as intralesional fat in myxoid liposarcoma, perilesional edema and a rim of fat in myxoma, and the swirled T2-weighted signal intensity and enhancement pattern of aggressive angiomyxoma, assist the radiologist in differentiating among these lesions. The presence of an internal chondroid matrix or incomplete peripheral ossification may suggest myxoid chondrosarcoma

or ossifying fibromyxoid tumor, respectively. The entering-and-exiting-nerve sign is suggestive of a peripheral nerve sheath tumor. Communication with a joint or tendon sheath and peripheral enhancement may indicate a ganglion or synovial cyst. In addition, the presence of multiple lesions suggests a syndrome, such as Mazabraud syndrome or neurofibromatosis. It is important to understand the imaging and pathologic features to prevent unnecessary biopsy of benign lesions and to ensure appropriate management of aggressive myxoid soft-tissue tumors.

Disclosures of Conflicts of Interest.—E.A.W.: Financial activities not related to the present article: consulting fees from Medical Metrics.

References

1. Graadt van Roggen JF, Hogendoorn PC, Fletcher CD. Myxoid tumours of soft tissue. *Histopathology* 1999;35(4):291–312.

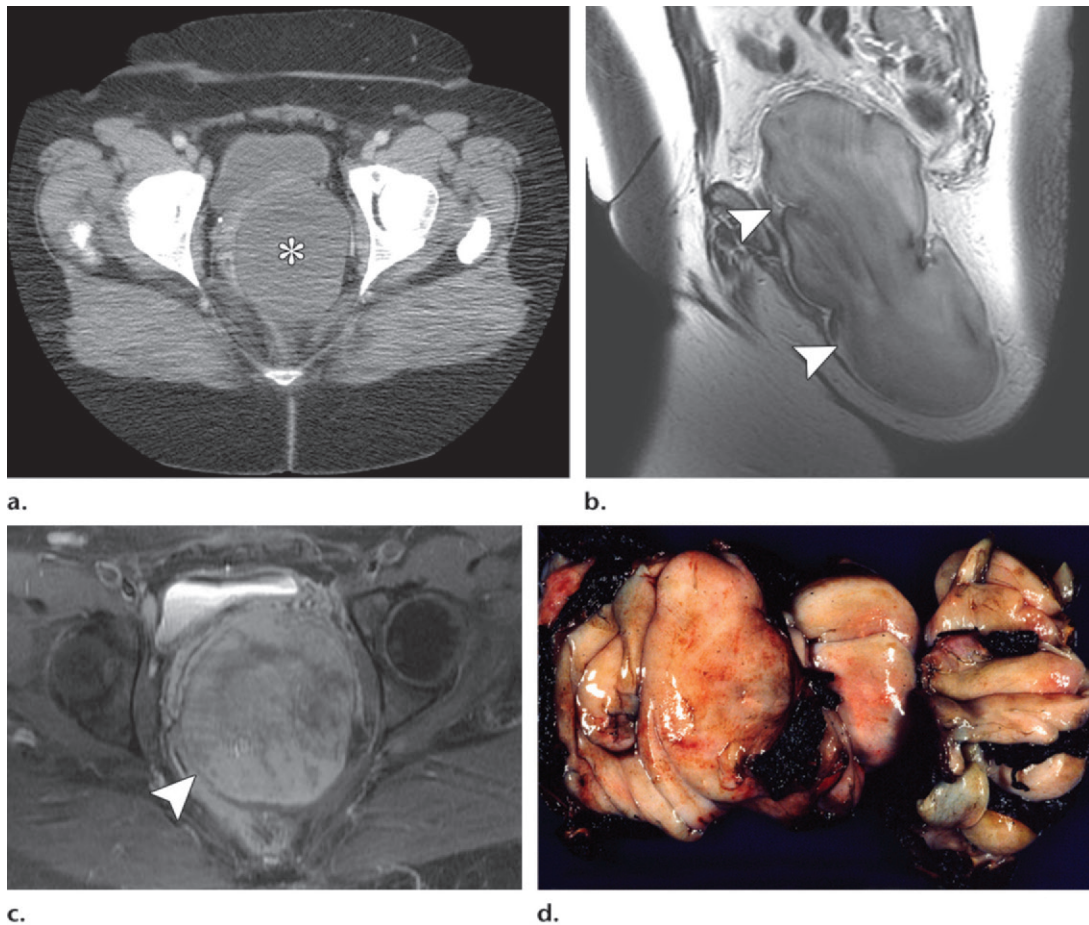
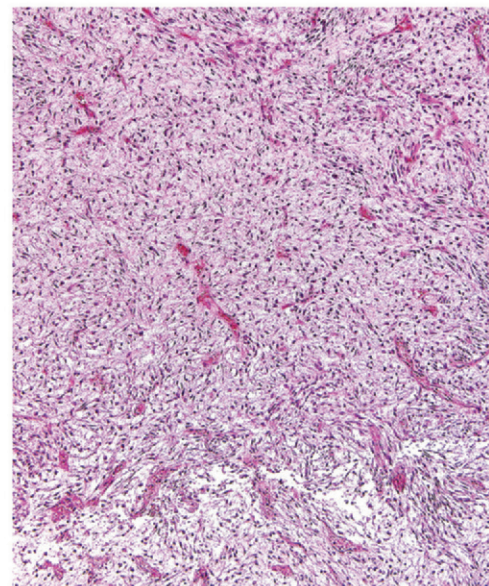


Figure 12. Aggressive angiomyxoma in a 64-year-old woman with an uncomfortable pelvic mass. **(a)** Axial CT image shows a pelvic mass (*) with attenuation less than that of skeletal muscle that is causing anterior displacement of the vagina and bladder. **(b)** Sagittal T2-weighted MR image (600/107) demonstrates a lesion (arrowheads) with heterogeneous intermediate signal intensity, showing the characteristic swirled or layering pattern of aggressive angiomyxoma. **(c)** Axial contrast-enhanced T1-weighted fat-suppressed MR image (550/7.9) shows a swirled pattern of enhancement within the lesion (arrowhead). **(d)** Photograph of the sectioned gross specimen. **(e)** Photomicrograph (original magnification, $\times 40$; H-E stain) shows stellate and spindle cells within a highly vascularized myxoid stroma.



e.

2. Stout AP. Myxoma, the tumor of primitive mesenchyme. *Ann Surg* 1948;127(4):706–719.
3. Kransdorf MJ, Murphey M. Imaging of soft tissue tumors. 2nd ed. Philadelphia, Pa: Lippincott Williams & Wilkins, 2006; 320.
4. Fletcher CD, Unni KK, Mertens F. Pathology and genetics of tumours of soft tissue and bone (IARC WHO classification of tumours). 3rd ed. Geneva, Switzerland: World Health Organization, 2006;186.
5. Weiss SW, Goldblum JR, Folpe AL, eds. Enzinger and Weiss's soft tissue tumors. 5th ed. Philadelphia, Pa: Mosby Elsevier, 2007; 1425.
6. Murphey MD, McRae GA, Fanburg-Smith JC, Temple HT, Levine AM, Aboulafla AJ. Imaging of soft-tissue myxoma with emphasis on CT and MR

- and comparison of radiologic and pathologic findings. *Radiology* 2002;225(1):215–224.
7. Kransdorf MJ, Murphey MD. Diagnosis please: case 12—Mazabraud syndrome. *Radiology* 1999; 212(1):129–132.
8. Walker EA, Fenton ME, Salesky JS, Murphey MD. Magnetic resonance imaging of benign soft tissue neoplasms in adults. *Radiol Clin North Am* 2011; 49(6):1197–1217, vi.

9. Pettersson H, Hudson TM, Springfield DS, Kaude JV. Cystic intramuscular myxoma: report of a case. *Acta Radiol Diagn (Stockh)* 1985;26(4):425-426.
10. Kransdorf MJ, Moser RP Jr, Jelinek JS, Weiss SW, Buetow PC, Berrey BH. Intramuscular myxoma: MR features. *J Comput Assist Tomogr* 1989;13(5):836-839.
11. Fornage BD, Romsdahl MM. Intramuscular myxoma: sonographic appearance and sonographically guided needle biopsy. *J Ultrasound Med* 1994;13(2):91-94.
12. Girish G, Jamadar DA, Landry D, et al. Sonography of intramuscular myxomas: the bright rim and bright cap signs. *J Ultrasound Med* 2006;25(7):865-869; quiz 870-871.
13. Bancroft LW, Kransdorf MJ, Menke DM, O'Connor MI, Foster WC. Intramuscular myxoma: characteristic MR imaging features. *AJR Am J Roentgenol* 2002;178(5):1255-1259.
14. Iwasko N, Steinbach LS, Disler D, et al. Imaging findings in Mazabraud's syndrome: seven new cases. *Skeletal Radiol* 2002;31(2):81-87.
15. Luna A, Martinez S, Bossen E. Magnetic resonance imaging of intramuscular myxoma with histological comparison and a review of the literature. *Skeletal Radiol* 2005;34(1):19-28.
16. Weiss SW, Goldblum JR. Benign tumors of peripheral nerves. In: Weiss SW, Goldblum JR, Folpe AL, eds. *Enzinger and Weiss's soft tissue tumors*. 5th ed. Philadelphia, Pa: Mosby Elsevier, 2007; 825-901.
17. Kransdorf MJ. Benign soft-tissue tumors in a large referral population: distribution of specific diagnoses by age, sex, and location. *AJR Am J Roentgenol* 1995;164(2):395-402.
18. Miettinen MM. *Diagnostic soft tissue pathology*. New York, NY: Churchill Livingstone, 2002; 608.
19. Ogose A, Hotta T, Morita T, Otsuka H, Hirata Y. Multiple schwannomas in the peripheral nerves. *J Bone Joint Surg Br* 1998;80(4):657-661.
20. Sheikh S, Gomes M, Montgomery E. Multiple plexiform schwannomas in a patient with neurofibromatosis. *J Thorac Cardiovasc Surg* 1998;115(1):240-242.
21. Beggs I. Sonographic appearances of nerve tumors. *J Clin Ultrasound* 1999;27(7):363-368.
22. Reinbold WD, Wimmer B, Adler CP, Genant HK. Radiologic findings in peripheral neurilemoma. *Eur J Radiol* 1987;7(4):268-273.
23. Fortman BJ, Kuszyk BS, Urban BA, Fishman EK. Neurofibromatosis type 1: a diagnostic mimicker at CT. *RadioGraphics* 2001;21(3):601-612.
24. Banks KP. The target sign: extremity. *Radiology* 2005;234(3):899-900.
25. Jee WH, Oh SN, McCauley T, et al. Extraaxial neurofibromas versus neurilemmomas: discrimination with MRI. *AJR Am J Roentgenol* 2004;183(3):629-633.
26. Cohen LM, Schwartz AM, Rockoff SD. Benign schwannomas: pathologic basis for CT inhomogeneities. *AJR Am J Roentgenol* 1986;147(1):141-143.
27. Walker EA, Song AJ, Murphey MD. Magnetic resonance imaging of soft-tissue masses. *Semin Roentgenol* 2010;45(4):277-297.
28. Conrad EU 3rd, Enneking WF. Common soft tissue tumors. *Clin Symp* 1990;42(1):2-32.
29. Weiss SW, Goldblum JR. Benign tumors and tumor-like lesions of synovial tissue. In: Weiss SW, Goldblum JR, Folpe AL, eds. *Enzinger and Weiss's soft tissue tumors*. 5th ed. Philadelphia, Pa: Mosby Elsevier, 2007; 1444.
30. Cardinal E, Buckwalter KA, Braunstein EM, Mih AD. Occult dorsal carpal ganglion: comparison of US and MR imaging. *Radiology* 1994;193(1):259-262.
31. Haller J, Resnick D, Greenway G, et al. Juxta-articular ganglionic (or synovial) cysts: CT and MR features. *J Comput Assist Tomogr* 1989;13(6):976-983.
32. Hashimoto BE, Hayes AS, Ager JD. Sonographic diagnosis and treatment of ganglion cysts causing suprascapular nerve entrapment. *J Ultrasound Med* 1994;13(9):671-674.
33. Feldman F, Singson RD, Staron RB. Magnetic resonance imaging of para-articular and ectopic ganglia. *Skeletal Radiol* 1989;18(5):353-358.
34. Beaman FD, Peterson JJ. MR imaging of cysts, ganglia, and bursae about the knee. *Radiol Clin North Am* 2007;45(6):969-982, vi.
35. Fielding JR, Franklin PD, Kustan J. Popliteal cysts: a reassessment using magnetic resonance imaging. *Skeletal Radiol* 1991;20(6):433-435.
36. Sung MS, Kang HS, Suh JS, et al. Myxoid liposarcoma: appearance at MR imaging with histologic correlation. *RadioGraphics* 2000;20(4):1007-1019.
37. Walker EA, Salesky JS, Fenton ME, Murphey MD. Magnetic resonance imaging of malignant soft tissue neoplasms in the adult. *Radiol Clin North Am* 2011;49(6):1219-1234, vi.
38. Murphey MD, Arcara LK, Fanburg-Smith J. Imaging of musculoskeletal liposarcoma with radiologic-pathologic correlation. *RadioGraphics* 2005;25(5):1371-1395.
39. Mentzel T, Calonje E, Wadden C, et al. Myxofibrosarcoma: clinicopathologic analysis of 75 cases with emphasis on the low-grade variant. *Am J Surg Pathol* 1996;20(4):391-405.
40. Weiss SW, Goldblum JR, et al. Malignant fibrous histiocytoma (pleomorphic undifferentiated sarcoma). In: Weiss SW, Goldblum JR, Folpe AL, eds. *Enzinger and Weiss's soft tissue tumors*. 5th ed. Philadelphia, Pa: Mosby Elsevier, 2007; 403-426.
41. Mansoor A, White CR Jr. Myxofibrosarcoma presenting in the skin: clinicopathological features and differential diagnosis with cutaneous myxoid neoplasms. *Am J Dermatopathol* 2003;25(4):281-286.
42. Smith MT, Farinacci CJ, Carpenter HA, Bannayan GA. Extraskelletal myxoid chondrosarcoma: a clinicopathological study. *Cancer* 1976;37(2):821-827.
43. Tsuneyoshi M, Enjoji M, Iwasaki H, Shinohara N. Extraskelletal myxoid chondrosarcoma: a clinicopathologic and electron microscopic study. *Acta Pathol Jpn* 1981;31(3):439-447.
44. Murphey MD, Walker EA, Wilson AJ, Kransdorf MJ, Temple HT, Gannon FH. Imaging of primary chondrosarcoma: radiologic-pathologic correlation. *RadioGraphics* 2003;23(5):1245-1278.
45. Weiss SW. Ultrastructure of the so-called "chordoid sarcoma": evidence supporting cartilagenous differentiation. *Cancer* 1976;37(1):300-306.
46. Meis-Kindblom JM, Bergh P, Gunterberg B, Kindblom LG. Extraskelletal myxoid chondrosarcoma: a reappraisal of its morphologic spectrum and prognostic factors based on 117 cases. *Am J Surg Pathol* 1999;23(6):636-650.
47. Oliveira AM, Sebo TJ, McGrory JE, Gaffey TA, Rock MG, Nascimento AG. Extraskelletal myxoid chondrosarcoma: a clinicopathologic, immunohistochemical, and ploidy analysis of 23 cases. *Mod Pathol* 2000;13(8):900-908.

48. Drilon AD, Popat S, Bhuchar G, et al. Extraskeletal myxoid chondrosarcoma: a retrospective review from 2 referral centers emphasizing long-term outcomes with surgery and chemotherapy. *Cancer* 2008;113(12):3364–3371.
49. Whitten CG, el-Khoury GY, Benda JA, Ehara S. Case report 829: intramuscular myxoid chondrosarcoma. *Skeletal Radiol* 1994;23(2):153–156.
50. Tateishi U, Hasegawa T, Nojima T, Takegami T, Arai Y. MRI features of extraskeletal myxoid chondrosarcoma. *Skeletal Radiol* 2006;35(1):27–33.
51. Enzinger FM, Shiraki M. Extraskeletal myxoid chondrosarcoma: an analysis of 34 cases. *Hum Pathol* 1972;3(3):421–435.
52. Rubin BP, Fletcher CD. Myxoid leiomyosarcoma of soft tissue: an underrecognized variant [abstr]. *Mod Pathol* 1999;12:15A.
53. Holland JF, Bast RC Jr, Morton DL, Frei E III. *Cancer medicine*. 4th ed. Baltimore, Md: Williams & Wilkins, 1996; 830.
54. Cruz M, Murakami T, Tsuda K, et al. Myxoid leiomyoma of the uterus: CT and MRI features. *Abdom Imaging* 2001;26(1):98–101.
55. Enzinger FM, Weiss SW, Liang CY. Ossifying fibromyxoid tumor of soft parts: a clinicopathological analysis of 59 cases. *Am J Surg Pathol* 1989;13(10):817–827.
56. Miettinen M. Ossifying fibromyxoid tumor of soft parts: additional observations of a distinctive soft tissue tumor. *Am J Clin Pathol* 1991;95(2):142–149.
57. Ideta S, Nishio J, Aoki M, et al. Imaging findings of ossifying fibromyxoid tumor with histopathological correlation: a case report. *Oncol Lett* 2013;5(4):1301–1304.
58. Ogose A, Otsuka H, Morita T, Kobayashi H, Hirata Y. Ossifying fibromyxoid tumor resembling parosteal osteosarcoma. *Skeletal Radiol* 1998;27(10):578–580.
59. Cha JH, Kwon JW, Cho EY, Lee CS, Yoon YC, Choi SH. Ossifying fibromyxoid tumor invading the spine: a case report and review of the literature. *Skeletal Radiol* 2008;37(12):1137–1140.
60. Schaffler G, Raith J, Ranner G, Weybora W, Jeserschek R. Radiographic appearance of an ossifying fibromyxoid tumor of soft parts. *Skeletal Radiol* 1997;26(10):615–618.
61. Outwater EK, Marchetto BE, Wagner BJ, Siegelman ES. Aggressive angiomyxoma: findings on CT and MR imaging. *AJR Am J Roentgenol* 1999;172(2):435–438.
62. Fetsch JF, Laskin WB, Lefkowitz M, Kindblom LG, Meis-Kindblom JM. Aggressive angiomyxoma: a clinicopathologic study of 29 female patients. *Cancer* 1996;78(1):79–90.
63. Yaghoobian J, Zinn D, Ramanathan K, Pinck RL, Hilfer J. Ultrasound and computed tomographic findings in aggressive angiomyxoma of the uterine cervix. *J Ultrasound Med* 1987;6(4):209–212.
64. Amr SS, el-Mallah KO. Aggressive angiomyxoma of the vagina. *Int J Gynaecol Obstet* 1995;48(2):207–210.
65. Smith HO, Worrell RV, Smith AY, Dorin MH, Rosenberg RD, Bartow SA. Aggressive angiomyxoma of the female pelvis and perineum: review of the literature. *Gynecol Oncol* 1991;42(1):79–85.
66. Destian S, Ritchie WG. Aggressive angiomyxoma: CT appearance. *Am J Gastroenterol* 1986;81(8):711–713.
67. Kobayashi Y, Minami M, Ohtomo K, Matsuoka Y. MR imaging and CT appearances of aggressive angiomyxoma. *AJR Am J Roentgenol* 1997;169(6):1752–1753.

Soft-Tissue Myxomatous Lesions: Review of Salient Imaging Features with Pathologic Comparison

Jonelle M. Petscavage-Thomas, MD, MPH • Eric A. Walker, MD • Chika I. Logie, MD • Loren E. Clarke, MD • Dennis M. Duryea, DO • Mark D. Murphey, MD

RadioGraphics 2014; 34:964–980 • Published online 10.1148/rg.344130110 • Content Codes:    

Page 965

A sonographic bright rim sign of increased echogenicity is often noted (in 83% of cases) around the myxoma, which is similar to the rind of fatty tissue around intramuscular myxoma described for MR imaging later. Also frequently noted is the bright cap sign, a triangular hyperechoic area adjacent to at least one of the poles of the mass (12) that corresponds to more prominent adipose tissue at the poles of the lesion.

Page 968

The target sign is commonly seen in neurofibroma (58%) but can also be detected in schwannoma (15%). This sign refers to low to intermediate T2-weighted signal intensity located centrally secondary to fibrous tissue with a higher collagen content and high T2-weighted signal intensity located peripherally, probably related to myxoid (high water content) tissue (24). If the peripheral myxoid component is predominant, the lesion may be confused with other myxoid lesions, particularly on images obtained with fluid-sensitive sequences.

Page 972

The pathognomonic feature of myxoid liposarcoma on MR images is identification of a fatty component within the mass, best seen as foci with high signal intensity on T1-weighted images, usually appearing lacy or linear and amorphous, rather than solid. These foci appear to have intermediate signal intensity with fat-suppressed or short inversion time inversion-recovery sequences (16). MR imaging is superior to CT for the detection of fat because of greater soft-tissue contrast resolution.

Page 974

Myxofibrosarcoma is most difficult to distinguish from myxoid liposarcoma. Hemorrhage on T1-weighted images may mimic intralesional fat but has high signal intensity on T1-weighted fat-suppressed images.

Page 976

Aggressive angiomyxoma may demonstrate swirled or layering tissue, seen best with sagittal T2-weighted MR sequences (Fig 12b) but also noted at CT and T1-weighted MR imaging after administration of contrast material (83%), resulting in a distinctive appearance (Fig 12c) (3,61).